LHC Project Note 71

1996-11-06
(Bosser@ps.msm.cern.ch)

Preliminary Measurements on Microcalorimeters foreseen to be used as Beam-loss Monitors

J. Bosser (PS–BD), H. Bouyaya (LHC–Ent.), G. Ferioli (SL–BI), B. Jenninger (LHC–ECR), Ch. Policella (LHC–ECR), J.M. Rieubland (LHC–ECR), A. Rijllart (LHC–IAS)

Summary

Preliminary measurements have been made with microcalorimeters in view of their possible use as beam-loss monitors for the LHC. The devices themselves are derived from those in use on some of the LEP magnets [Ph. Lebrun et al., CERN AT/92–18(CR-MA)]. A carbon resistance, acting as a thermometer, is thermally coupled to a copper block, initially at the cryostat temperature. As a result of high-energy particle losses the resulting shower will deposit heat into the copper. The measurement of the resistance decrease as a result of the copper temperature increase is expected to provide a means of estimating the number of particles lost. Laboratory tests and measurements made with SPS extracted beams are reported in this note.

1 Introduction

We report on some preliminary measurements made in the laboratory and with an extracted proton beam, for a new type of beam-loss monitor intended to be used as part of the LHC machine diagnostics.

The beam-loss monitors are ‘microcalorimeters’ as described in Refs. [1],[2]. The particles lost by the circulating proton beam deposit part of their energy in a copper block which is initially at the magnet temperature (1.9 K). Thermally coupled to the copper block, acting as a thermometer, is a carbon resistance R [Ω] manufactured by Allen-Bradley. Indeed as a consequence of the losses, and therefore of the increase in temperature of the copper, the resistance R is heated and its value is thus decreased. The measurement of the resistance value should enable us to determine, at least in a relative manner, the amount of protons lost.

The ensemble ‘copper + resistance’ is called a microcalorimeter or more simply ‘mucal’.

For particle losses in the LHC one can foresee two distinct cases:

- Losses which occur during a short interval of time, of the order of a few milliseconds. The heat pulse is supposed to be relatively dense and the mucal is expected to have a short time response.
- Continuous losses for at least several seconds. The mucal is expected to be more sensitive in the pulsed case with, however, larger time constants.

For our purpose we built a simple small cryogenic vessel, or cryostat, coupled to a 100 l He Dewar. The cryostat should provide the required temperature of about 1.9 K to the calorimeters placed inside of it under a vacuum pressure lower than 10^{-6} mbar. The calorimeters have different volumes and use different 'thermometer resistances'.

First we used calorimeters having the same mechanical arrangement as that reported in Ref. [1] and tested them with protons extracted in the North-H6 beam line of the SPS. We then built a new type of microcalorimeter which was first tested in the laboratory and then on the extracted proton beam line. Both type of measurements, in the laboratory and with extracted beams, will be reported on in this note.

2 Laboratory measurements

2.1 Cryostat design

The cryostat is used to cool a metallic plate, onto which the calorimeters are laid, down to the required temperature.

The cryostat contains its own He transfer line. It is fixed above a 100 l He Dewar and composed of the following components (Fig. 1):

- Liquid input line
- Separator
- Thermalization circuit for the wires and the thermal screen
- Thermal screen
- Expansion valve
- Evaporator and its pumping tube

All these components are placed inside a sealed vacuum environment with a pressure less than 10^{-6} mbar.

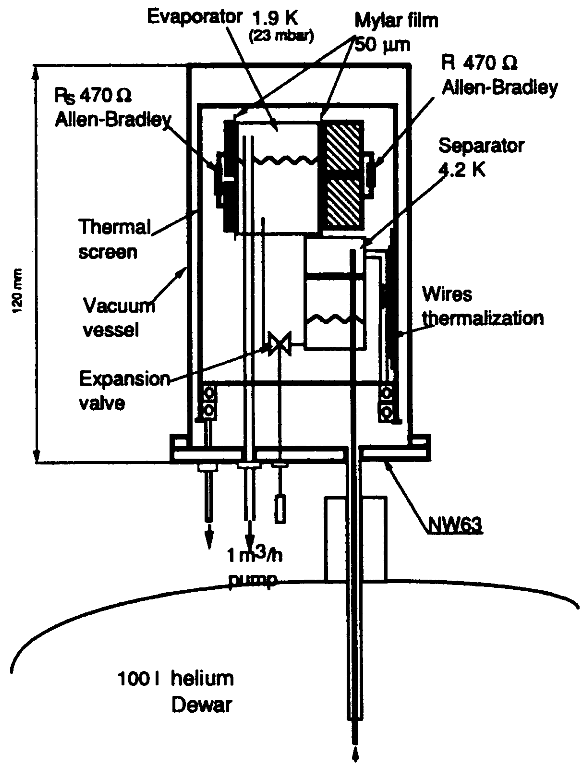

Fig. 1: Principle of the cryostat. The calorimeter represented is that described by Fig. 2; however, calorimeter types as described in Ref. [1] are also mounted within the same cryostat for tests.

2.1.1 *Principle of operation*

Owing to the Dewar pressure (50 mbar over atmospheric pressure) the liquid helium will be transferred towards the separator. At this level the 4.2 K gas is drained out through a circuit whose function is to cool the screen and the measuring wires (about 10 wires) to about 10 K.

At the bottom of the separator the liquid is sent, through a valve, into an evaporator where the actual pressure is 23 mbar and therefore the liquid is at 1.9 K. The role of the expansion valve is to bring the liquid pressure from its initial value (about 1000 mbar) to about 23 mbar and also to adjust the liquid level in the evaporator. The 23 mbar pressure level is obtained thanks to a vacuum pump (1 m^3/h) placed at the output of the pumping tube.

One of the difficulties is how to fix the copper blocks onto the cold source plate, at 1.9 K. If the resulting thermal resistance between the calorimeter copper block and the cold wall is too small then the thermometer will not be significantly heated as a result of beam losses. Conversely a too large resistance will transform the thermometer into a dosimeter.

2.1.2 *Main characteristics of the cryostat*

- Autonomy with a 100 l Dewar: ≅ 7 days
- Evaporator flow: ≅ 23 N·l/h
- Static losses on evaporator: ≅ 8 mW
- Screen flow: ≅ 300 N·l/h
- Screen temperature: ≅ 10 K
- Dimensions: diameter: 70 mm; height: 120 mm

2.2 Microcalorimeter design

The principle of the experimental set-up is shown in Fig. 2. A carbon type resistance 'R' is mechanically inserted between two half-cylinder copper blocks. The copper blocks are placed on the cold wall of the cryostat, at constant temperature: $T_{exp} \cong 1.9$ K, through a thin Mylar film. The values of the 'thermometer' resistances as a function of the temperature 'T', i.e. R = R (T), or conversely T (R), have always been measured prior to any experiment so that we have at our disposal the relation between the resistance and its temperature.

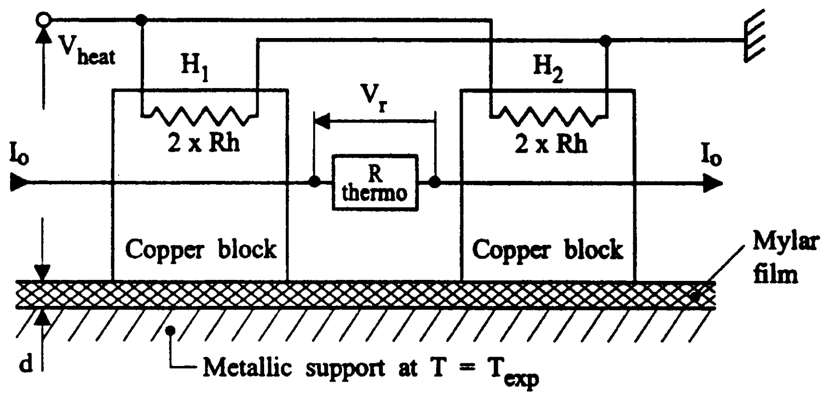

Fig. 2: Principle of the microcalorimeter tested in the laboratory and used during the second experiment with an extracted proton beam. H_1, H_2: heaters; R_h: heater resistance; R: thermometer resistance.

The laboratory measurements of $T(R)$ are fitted, within our temperature range, according to the following expression:

$$T\ (R) = \frac{B}{\left(\log(R) + \left(\frac{K}{\log(R)}\right) - A\right)} \qquad (1.a)$$

where the coefficients A, B and K depend on the type of resistance used.

Consequently:

$$R\ (T) = \exp\left[\frac{\ln(10)}{2 \cdot T} \cdot (T \cdot A + B + \sqrt{T^2 \cdot A^2 + 2 \cdot T \cdot A \cdot B + B^2 - 4 \cdot T^2 \cdot K})\right]. \qquad (1.b)$$

For the copper heating one can use the following equality:

$$\delta Q = m \cdot Cp \cdot \delta T$$

where m [g] is the copper mass, Q [J] is the heat and T [K] the temperature. The copper specific heat Cp [J/(g.K)] is expressed by:

$$Cp\ (T) = 10.8 \cdot 10^{-6} \cdot T + 30.6 \cdot \left(\frac{T}{344.5}\right)^3 .$$

For small temperature variations, or a small energy supply ΔQ [J/g], one can simply use:

$$\Delta Q = Cp \cdot \Delta T . \qquad (2)$$

A more accurate expression for the determination of the temperature increase is to determine the ΔT solution of:

$$\Delta Q = \int_{T_{ic}}^{T_{ic}+\Delta T} Cp\ (T) \cdot dT \qquad (3)$$

where T_{ic} is the copper block initial temperature.

On one face of each of the thermometer copper blocks, two heaters (H_1, H_2), each consisting of a strain gauge, have been installed. They heat the copper blocks in pulsed or continuous mode. The total heater resistance $R_{heat} \cong 50\ \Omega$.

The resistance and the copper blocks are traversed by a current I_o such that the voltage V_r across R will allow us to determine the value of the resistance and therefore its temperature. Nominally I_o is chosen so as not to heat significantly the 'copper–resistance' ensemble. However, an increase of I_o from its nominal value to about $10 \cdot I_o$ will be another way to modify the resistance temperature.

Inside the cryostat a second resistance R_s has been installed. The resistance R_s is identical to R, but associated with a smaller copper block volume free of any heater. Its purpose is to provide differential measurements and therefore to obtain more accurate measurements of R. In the present case this 'second' resistance showed, for the same T_{exp}, higher values than the thermometer one (i.e. R). This leads us to suspect that, because of the heaters and of the power radiated by the thermal screen, at 10 K, on the large copper surface associated with R, the thermalization is not perfect and has to be improved in future experiments. The resistance R_s has, however, been used for relative measurements.

It is worth keeping in mind that, owing to the Mylar film and the presence of wires and heaters, though T_{exp} is the temperature of the metallic support, the nominal (i.e. without any additional heat supply) temperature of R and R_s might be larger than T_{exp}. However, in what follows R (T_{exp}) or R_s (T_{exp}) will express the resistance values when the metallic wall is T_{exp} and we are not concerned with the extra heat.

The principle of the electronic measurement set-up is shown in the upper part of Fig. 3 where R_{out} placed outside the cryostat allows us to observe I_0. Anticipating on experiments made with extracted proton beams (which will be described in Section 3), the lower part of Fig. 3 represents the principle of the spill and integrated spill measurements.

The electrical circuit approximately equivalent to the actual thermodynamic system is represented by Fig. 4. Some of the set-up parameters are reported in Table 1.

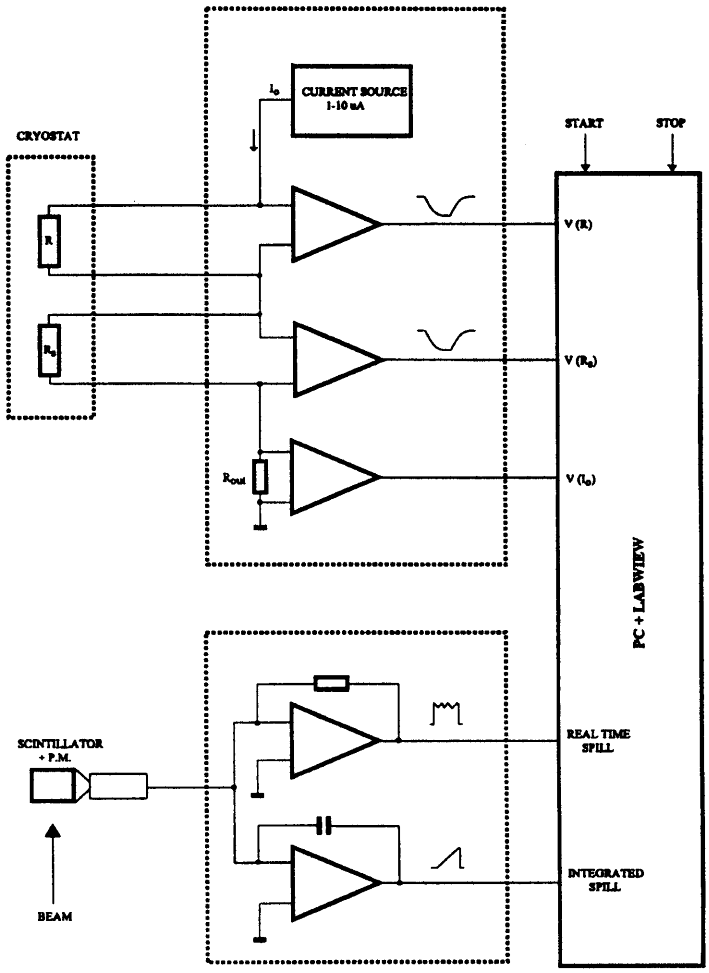

Fig. 3: Principle of the electrical set-up.

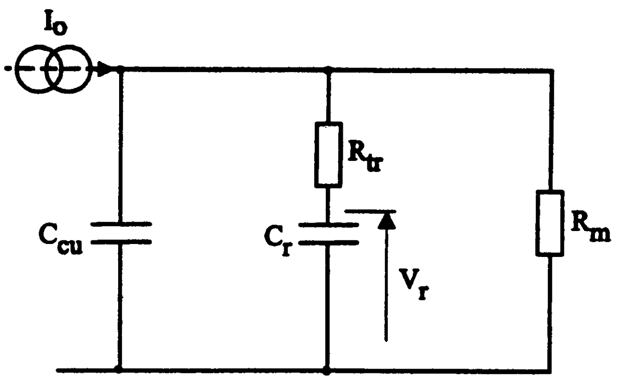

Fig. 4: Electrical circuit equivalent to the thermodynamic system. C_{cu} ≡ Copper block heat capacity; C_r ≡ carbon resistance (or R) heat capacity; R_{tr} ≡ thermal resistance between the copper blocks and the resistance R; R_m ≡ thermal resistance between the copper blocks and the cold mass at temperature T_{exp}; I_o ≡ heat intensity Q [J/s or J/(g·s)].

Table 1
Main microcalorimeter parameters

Copper block dimensions [cm]	Half-diameter = 1.5; length = 2 for R and length = 0.3 for R_s
Copper density [g/cm^3]	8.96
Copper mass: m_{cu} [g]	126.67 for R, 19 for R_s
Heater resistance R_h [Ω]	50
Mylar insulation thickness d [μm]	50
Resistance nominal current I_o [μA]	1
Cryostat experimental temperature: T_{exp} [K]	1.9

2.3 Type of laboratory measurements

Three types of measurements have been made on different resistances.

- First experiment: A voltage pulse V_{heat} is applied on the heaters for time t = 10 ms. This is equivalent to a pulsed loss of particles. As will be seen the pulse duration is less than the observed resistance heating time which is of the order of 100 ms. Figure 5 is an example of the measured $V(t)$ on $R = R_1$ (refer to Section 2.4 for the definition of $R = R_1$).
- Second experiment: V_{heat} is applied on the heaters for about 4.5 s. This should be equivalent to a continuous proton beam loss. Figure 6 shows $V(t)$ as measured on $R = R_3$ (refer to Section 2.4).
- Third experiment: We increased I_o from 1 μA to about 10 μA for a short time during which R is heated. Once the current has reverted to its initial values I_o = 1 μA, the resistance cools down to its initial temperature. One of the plots of $V(t)$ as measured with: $R = R_4$ (refer to Section 2.4), is given by Fig. 7.

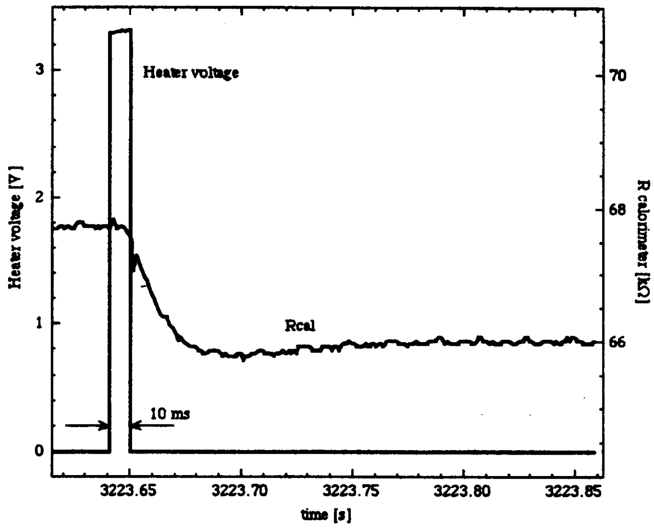

Fig. 5: Thermometer resistance R (t) as a function of time in response to a pulse: V_{heat} [V] scaled on the left vertical axis. $R \equiv R_1$. Right vertical axis: R [kΩ]. Horizontal axis: time t [s].

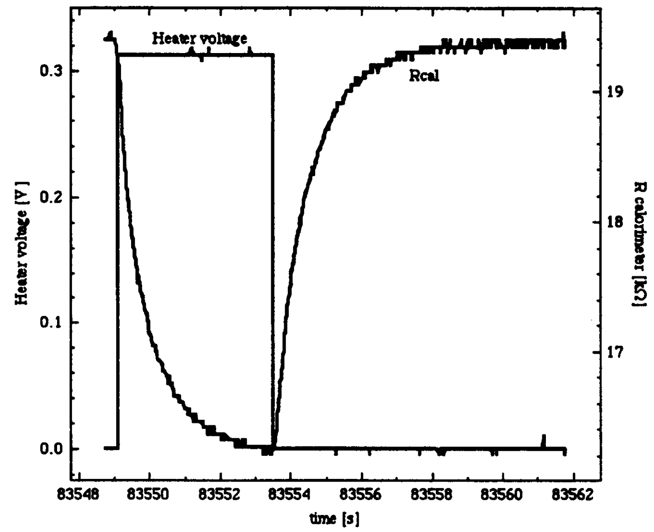

Fig. 6: Thermometer resistance R (t) as a function of time in response to a constant voltage applied on the heater. The resistance type is $R \equiv R_3$. Left vertical axis: V_{heat} [V]. Right vertical axis: R [kΩ]. Horizontal axis: time t [s].

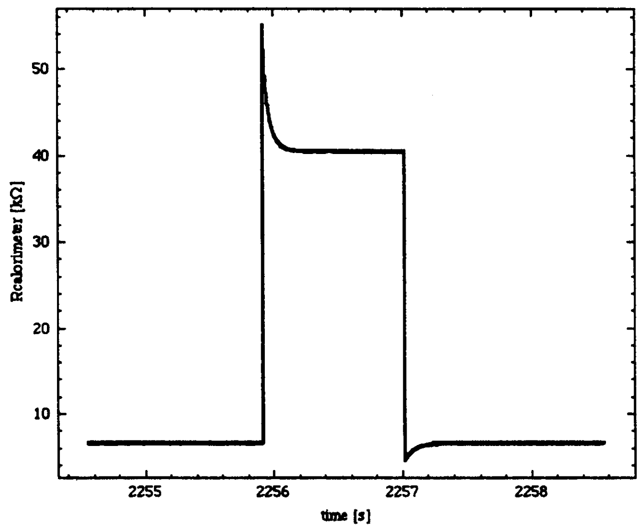

Fig. 7: Time response of the thermometer resistance after pulsing I_0 from 1 μA to 10 μA for 1 s. $R \equiv R_4$. Vertical axis: R [kΩ]. Horizontal axis: time t [s].

All the experiments have been checked on an oscilloscope and then the data acquired and processed using 'LabVIEW'. Of course dedicated electronics and coding have been developed for each type of experiment (this also includes the experiments made with a proton beam which will be described later on).

2.4 Results of the measurements

We used different types of thermometer resistances R namely:

a) R_1: $R_1 = 150\ \Omega$, 2 W at room temperature. $R_1\ (T_{exp}) = 60\ 000\ \Omega$.

b) R_2: $R_2 = 180\ \Omega$, 1/8 W at room temperature. $R_2\ (T_{exp}) = 12\ 400\ \Omega$. We intend in this case to benefit from a reduced dimension (with respect to R_1) thermometer and therefore a reduced resistor thermal capacity (C_r of Fig. 4). The expected faster response time is, however, counterbalanced by the fact that the resistance value is quite small and that the reduced connecting wire diameter will induce an increase of the thermal resistance between the copper blocks and the thermometer resistance itself (R_{tr} on Fig. 4). More precisely the product $C_r \cdot R_{tr}$ [s] (Fig. 4) remains constant.

c) R_3: $R_3 = 220\ \Omega$, 1/8 W at room temperature. $R_3\ (T_{exp}) = 19\ 550\ \Omega$. R_3 was filed down on the outside so as to reduce its encapsulation volume (and therefore its thermal capacity).

d) R_4: $R_4 = 380\ \Omega$, 1/8 W at room temperature. $R_4\ (T_{exp}) = 59\ 000\ \Omega$. The wires which connect the copper blocks to the resistance were soldered instead of being pinched as was the case for the previous resistances (a), (b) and (c). The numbers referring to this resistance, later in this paragraph, must be reduced by a factor of about 1.4 since we operate at $T_{exp} = 1.8$ K instead of 1.9 K.

e) R_5: $R_5 = 470\ \Omega$, 1/8 W at room temperature. $R_5\ (T_{exp}) = 67.4\ \text{k}\Omega$. This type of resistance was the one used during our second experiment with extracted proton beam (see Section 3.2). The measured values $R_5\ (T)$ require that Eq. (1) should be used with: $A = 8.420642$, $B = 0.552593$, and $K = 18.57672$.

2.4.1 First experiment

Heater powered for 10 ms. The symbol ΔR_{max} refers to the maximum resistance variation.

V_{heat} [V]	Heater energy [mJ]	$\Delta R_{1\ max}$ [Ω]	$\Delta R_{2\ max}$ [Ω]	$\Delta R_{3\ max}$ [Ω]	$\Delta R_{4\ max}$ [Ω]	$\Delta R_{5\ max}$ [Ω]
3.0	1.8	2000	2250	3600	18 000	17 500
2.0	0.8		900	1700		
1.5	0.45	450		800	6000	5400
0.8	0.128			300	1500	800
0.4	0.032		≅ 50	≅ 80	≅ 200	≅ 300

Note: For $V_{heat} = 0.4$ V we obtained poor accuracy in our measurements.

The heating and cooling times from 10% to 90% when $V_{heat} = 3$ V are as follows:

	R_1	R_2	R_3	R_4	R_5
Heating time [ms]	50	100	100	100	80
Cooling time [s]	3	3	3	3	2

2.4.2 *Second experiment*

Continuous powering of the heater for 4.5 s. We measured the thermometer asymptotic variation ΔR.

V_{heat} [mV]	Power [μW]	ΔR_1 [Ω]	ΔR_2 [Ω]	ΔR_3 [Ω]	ΔR_4 [Ω]	ΔR_5 [Ω]
320	2000	3000	3000	3200	22 000	17 800
260	1350	1800				
160	512	700	900	900	7000	5000
65	85	≅ 100	≅ 100	≅ 150	≅ 1200	≅ 800

For the present type of experiment the heating time is between 3 and 4 s and the cooling time about 3 s for any type of resistance. The heating time constant is estimated to be $\tau_h = 3/5 = 0.6$ s.

2.4.2.1 *More on temperature and resistance variations*

Let us focus on R_5 only for which we have given in Section 2.4 (e) the coefficients to be used in Eqs. (1). Initially $R_5\,(T_{exp}) = 67.4$ kΩ such that its initial temperature $T_i = T\,(67\,400\ \Omega) = 2.165$ K. Once we know the heating power $\Delta\dot{Q}$ [J/s]/(m_{cu} [g]), deposited in the copper blocks, we know from Ref. [2] that the amount of stored energy is ΔQ [J/g] $= \tau_h \cdot \dot{Q}$. Then using Eq. (3), with $T_{ic} = T_i$, one can compute the theoretical final temperature $T_{fth} = T_i + \Delta T_{th}$ and then with Eq. (1.b) obtain the theoretical final resistance $R_{fth} = R\,(T_{fth})$ and therefore the expected resistance variation. As an example using the data of the previous table:

- For $\Delta\dot{Q} = 2000 \cdot 10^{-6} / 126.67$ J/g·s one computes: $T_{fth} = 2.572$ K or $\Delta T_{th} = 0.275$ K, $R_{fth} = 46.1$ kΩ or a theoretical resistance variation $\Delta R_{th} = (R5 - R_{fth}) = 21.2$ kΩ. In practice we measured a final resistance $R_{fm} = 67\,400 - 17\,800 = 49\,600$ Ω which corresponds to a final 'measured' temperature $T_{fm} = 2.391$ K or a 'measured' temperature variation $\Delta T_m = (T_{fm} - T_i) = 0.225$ K to be compared with ΔT_{th}.
- For $\Delta\dot{Q} = 512 \cdot 10^{-6} / 126.67$ J/g·s one computes: $T_{fth} = 2.244$ K, $\Delta T_{th} = 0.079$ K, $R_{fth} = 60.7$ kΩ, $\Delta R_{th} = 6.7$ kΩ instead of a measured $\Delta R_m = 5$ kΩ, $T_{fm} = 2.233$ K, and $\Delta T_{fm} = 0.058$ K to be compared with ΔT_{th}.

The theoretical expectations and the measurements are in good agreement. The same applies to the other resistances. One can conclude that this type of measurement gives reliable results.

2.4.3 *Third experiment*

Thermometer heating by pulsing I_0 from 1 μA to 10 μA for about 2 s. The corresponding heating power is $P = R\ (T_{exp}) \times 10^{-10}$ W.

ΔR_1 [Ω]	ΔR_2 [Ω]	ΔR_3 [Ω]	ΔR_4 [Ω]	ΔR_5 [Ω]
12 000	1162	3200	14 000	14 000

P_1 [μW]	P_2 [μW]	P_3 [μW]	P_4 [μW]	P_5 [μW]
6	1.25	2	6	6

The heating and cooling times were about 150 ms whatever the resistance.

Let us consider R_5 the mass of which is expected to be 1 g. The measured ΔR is about the same as that given in Section 2.4.2 for $V_{heat} = 330$ mV. The actual power involved in this experiment is $P \cong 67.4 \cdot 10^3 \cdot 10^{-10} = 6.74 \cdot 10^{-6}$ [J/(g·s)] which is near to that involved in the previous experiments.

3 Tests with an extracted proton beam

The overall assembly (cryostat + microcalorimeter + Dewar) was installed in the H6 line of the SPS North extraction complex. The beam passing though this line consists mainly of a few 10^7 protons at about 120 GeV/*c*. The extracted spill has a duration of about 2.2 to 2.5 seconds.

The particle beam, of about 3 cm width and 1 cm height, was steered onto a cylindrical copper target which had the following dimensions: diameter = 5 cm, length = 50 cm. The microcalorimeters within the cryostat were placed at a distance of 50 cm from the target end (Fig. 8). The mucals were aligned as far as possible with the target, or beam axis. For our purpose we also used scintillators, coupled to a photomultiplier (not represented on Fig. 8).

These scintillators, calibrated by the experimentalists' intensity measurements, are used to record the extracted beam spill and its integral.

The energy deposited in the microcalorimeter block is given in Fig. 9 (G. Stevenson, private communication). From this figure one can state that on average:

- 1 to 2.10^{-10} J/kg, per proton impinging on the target, are deposited on the axis of the calorimeter copper block,
- $0.5 \cdot 10^{-10}$ J/kg, per proton impinging on the target, are deposited in the calorimeter copper block if placed 5 cm away from the target axis.

In the first experiment we used, without preliminary laboratory tests, the microcalorimeter type described (Ref. [1]). In this case the copper block is fixed onto the cold metallic wall (at $T_{exp} \cong 1.9$ K) while the thermometer resistance, embedded in the copper block, is electrically insulated from it.

In the second experiment we used the microcalorimeters as described in Section 2, namely with resistance $R \equiv R_5 \equiv R_s$ during all of this run. In principle (refer to Fig. 2) the copper blocks are electrically and thermally insulated from the cold cryostat wall by a Mylar foil, but thermally and electrically tightly coupled to the thermometer resistance R.

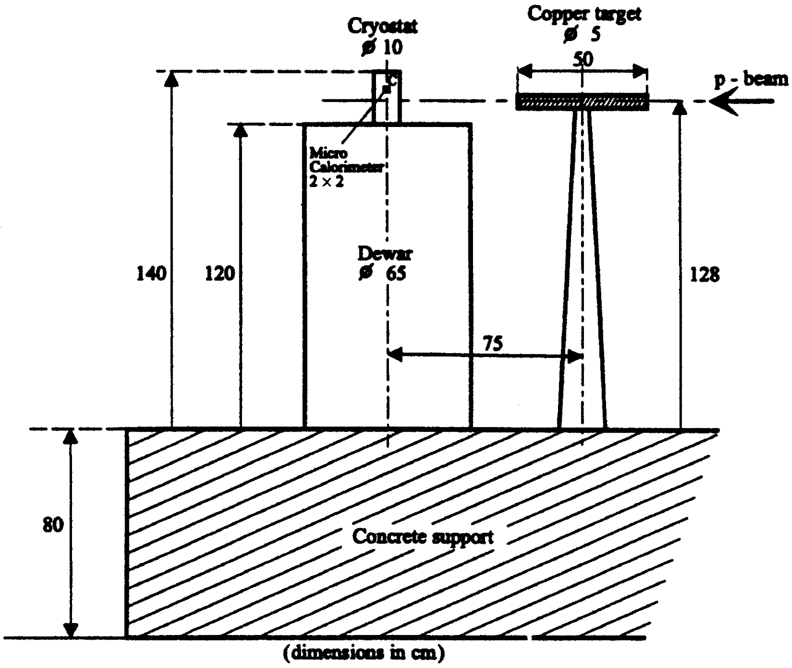

Fig. 8: Mechanical set-up of the experiments with an extracted proton beam.

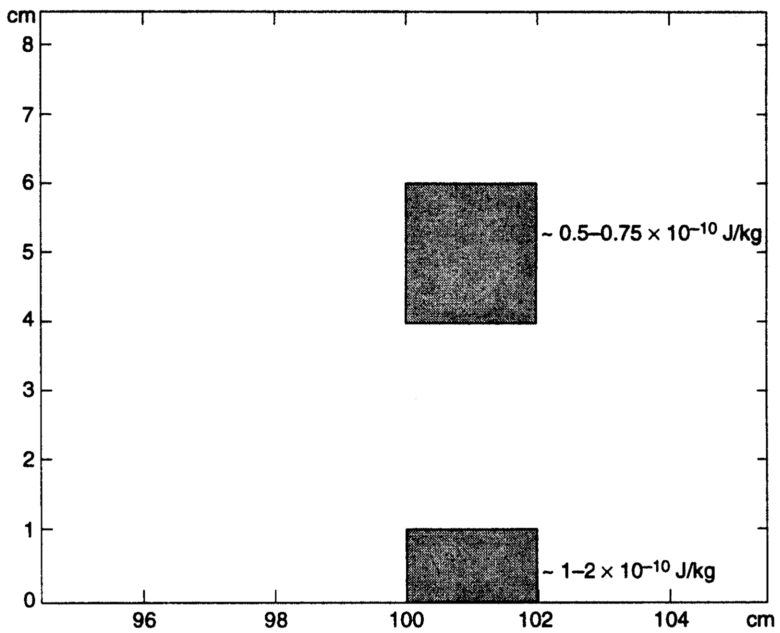

Fig. 9: Rough distribution of the deposited energy in the microcalorimeter copper block [J/kg·proton on the target]. The proton momentum at the copper target entrance is 120 GeV/c.

3.1 First experimental results

3.1.1 Type of microcalorimeter used

Inside the cryostat we placed three calorimeters, designed in accordance with the principle described in Ref. [1], but with some differences as follows:

- cal1: $R = 100\ \Omega$, 2 W (at ambient temperature) resistance within a copper block of volume $V = 2 \cdot 1 \cdot 2.6$ (length) $= 5.2\ \text{cm}^3$. The corresponding coefficients used in formula (1) are: $A = 3.400626$, $B = 3.450815$, $K = 2.768881$.
- cal2: $R = 100\ \Omega$, 1/8 W (at ambient temperature) resistance within a copper block of volume $V = 2 \cdot 1.6 \cdot 1$ (length) $= 3.2\ \text{cm}^3$.
- cal3: $R = 220\ \Omega$, 1/8 W (at ambient temperature) resistance in the copper ensemble as used for the LEP calorimeter [1], i.e. which has a volume of $1.8\ \text{cm}^3$.

For all of the three monitors we tried to thermalize, as much as possible, the connecting wires. All the resistances are connected in series with a nominal current of 1 μA flowing through them. No laboratory tests have been made on this type of microcalorimeters since they were not equipped with heaters.

3.1.2 Measurements

An illustration of our measurements is given by: Fig. 10(a) for cal1, Fig. 10(b) for cal2, and Fig. 10(c) for cal3. The vertical axis represents the number of protons (in units of 10^7) entering the target and the measured resistance R (in kΩ) as a function of the time t [s] represented on the horizontal axis.

Figure 11 shows a plot of the cal1 resistance $R(t)$ response over four SPS cycles.

From Fig. 10 it is obvious that cal1 is the most favourable for our purpose. The (1/e) rise or heating time constant is about 0.3 s like the (1/e) cooling time constant. The measured resistance variation $\Delta R = 33\,550 - 33\,250 = 300\ \Omega$. Using the calibration results $T(R)$ deduced from Eq. (1.a) (A, B, K are defined in Section 3.1.1) one estimates the corresponding temperatures: $T(33\,550\ \Omega) = 1.987$ K, $T(33\,250\ \Omega) = 1.991$ K, such that the measured resistance temperature increase, induced by about $2 \cdot 10^7$ protons/s, is 4 mK. This can be compared with the theoretical temperature increase of the copper block. In this case considering the calorimeter out of axis the deposited energy in the copper block is:

$$\Delta\dot{Q} = (0.5 \cdot 10^{-13}[\text{J/g} \cdot \text{proton}]) \cdot 2 \cdot 10^{7}[\text{protons/s}] = 10^{-6}[\text{J/g.s}]\ .$$

Taking a time constant $\tau = 0.27$ s we know from Ref. [2] that the final stored energy in copper volume is $\Delta Q\ [\text{J/g}] = \tau \cdot \Delta\dot{Q}$. Remembering Eq. (2): $\Delta Q = Cp \cdot \Delta T$, where the copper specific heat $Cp = 3 \cdot 10^{-5}$ J/(g·K), one obtains a theoretical temperature increase $\Delta T = 8$ mK.

a)

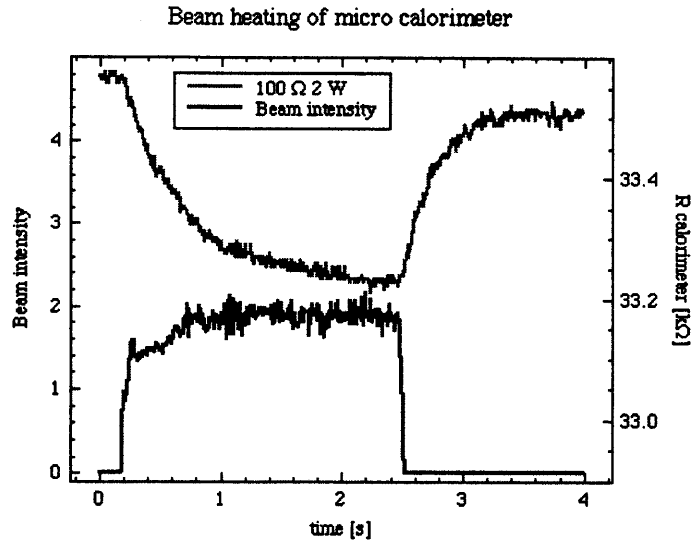

b)

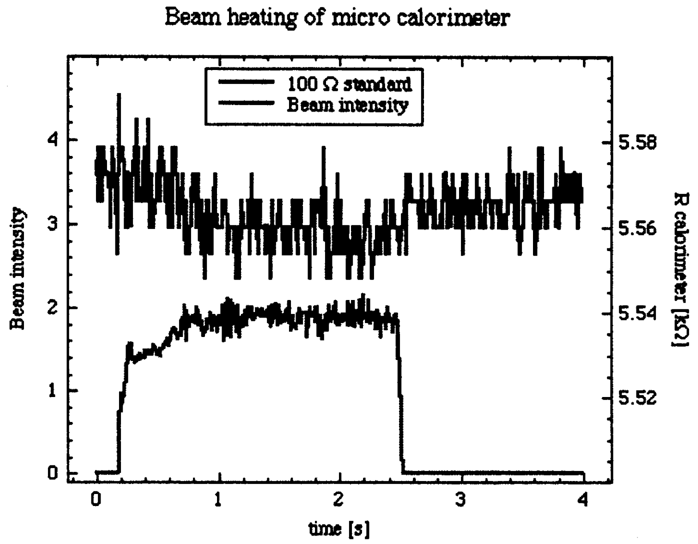

c)

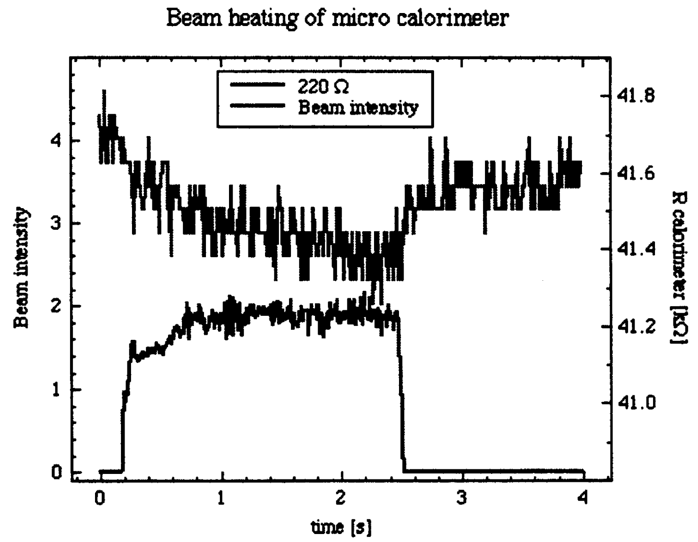

Fig. 10: Time response of the calorimeters to a proton spill on target. a) for cal1, b) for cal2, c) for cal3. Left vertical axis: number of protons on the target [in units of 10^7/s]. Right vertical axis: measured resistance [kΩ]. Horizontal axis: time t [s].

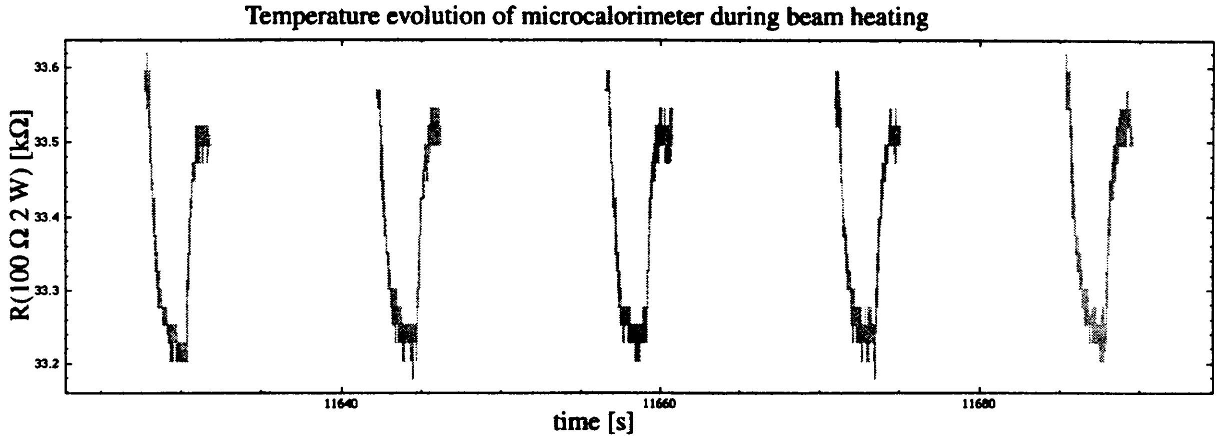

Fig. 11: Response of 'cal1' to five consecutive SPS extracted beams.

Our measurements show a calorimeter sensitivity reduced by a factor 2 with respect to the theoretical expected numbers. This has to be investigated and might be due to the relatively small copper volume and thermalization problems.

The relative sensitivity between cal1, cal2 and cal3 is supposed to result from:

- the relative measured $\mathrm{d}R/\mathrm{d}T|_{T=T_{exp}}$
- the ratio between the copper volumes.

3.2 Second experimental results

3.2.1 Type of microcalorimeter used

Inside the cryostat we installed the type of calorimeter described in Section 2 where the resistance used is the 'R_5' for both the thermometer R and the second resistance R_s (see Section 2.4; $A = 8.973051$, $B = 0.340594$, $K = 20.76258$). It is worth remembering that the copper volume associated with R_s is one-sixth of that associated with the thermometer (refer to Table 1). Both are off-axis by about 1–2 cm. Without any particle on the target the resistances are: $R\,(T_{exp}) = R_o = 66.2$ kΩ and $R_s\,(T_{exp}) = R_{so} = 107.5$ kΩ such that the actual initial temperatures are: $T_o\,(R) = T\,(R_o) = 2.179$ K and $T_{os}\,(R_s) = T\,(R_{so}) = 1.87$ K. An explanation of such a temperature difference has been given in Section 2.2.

3.2.2 Measurements

We measured, with or without the copper target, the evolution of the resistance and of the proton beam integrated spill, as a function of time, for various proton beam intensities. Samples of our measurements, when using the target, are given in:

- Figs. 12(a) and 12(b) when the integrated (over the spill time) number of protons on the target is $11.2 \cdot 10^7$. Figure 12(a) is relative to R while 12(b) is relative to R_s;
- Figs. 13(a) and 13(b) when the integrated number of protons on the target is $1.2 \cdot 10^7$ which implies a rate of: $1.2 \cdot 10^7$ p/2.2 [s] $\cong 5.5 \cdot 10^6$ p/s. Figure 13(a) is relative to R while 13(b) refers to R_s.

From Fig. 13(a) one can deduce that one could detect the heat induced by a proton beam whose intensity is reduced by a factor 4. From Fig. 13(b) one sees the effect of the acquisition system resolution which could be improved by a factor 4 (14 bits instead of the present 12 bits ADC) if compatible with the electronic system. As a consequence one can state that, in the present state of our calorimetric system, one could measure the induced energy lost by a proton beam whose intensity is reduced by a factor 16 (i.e. a rate of about $3.4 \cdot 10^5$ protons/s incident on the target). It must be stressed that in such a case the electronic system accuracy must be significantly improved since one must then be able to detect voltage variations, across the thermometer resistance, of about 60 μV.

The heating and cooling times can be deduced easily from Figs. 12 or 13. More precisely the dashed lines on Figs. 12(a) and 12(b) show that the time constants are about 1 s for R and 0.4 s for R_s. It can be clearly seen from the measurement that when using R_s one obtains lower resistance variation but smaller time constants (with respect to the measurements made with R).

A summary of our measurements is given in Tables 2 and 3.

Table 2

Measurements with proton beam but without target

Number N of protons $[10^7]$	$\log(N/10^7)$	R [kΩ]	$\log R$ $[10^4\Omega]$	ΔR [kΩ]	R_s [kΩ]	$\log(R_s)$ [kΩ]	ΔR_s [kΩ]
4.0	0.6	61.19	1.786	4.29	105.6	2.0236	1.9
9.4	0.973	60.89	1.784	5.31	104.7	2.0199	2.6
17.5	1.24	57.70	1.76	8.5	101.9	2.0081	5.6

Table 3

Measurements with proton beam and with target

Number N of protons $[10^7]$	$\log(N/10^7)$	R [kΩ]	$\log R$ [kΩ]	ΔR [kΩ]	R_s [kΩ]	$\log(R_s)$ [kΩ]	ΔR_s [kΩ]
1.2	0.0792	65.1	1.813	1.1	106.8	2.0285	0.7
2.5	0.3979	64.0	1.806	2.2	106.2	2.0261	1.3
3.4	0.5314	63.1	1.8	3.1	105.7	2.0240	1.8
6.6	0.8195	61.0	1.785	5.2	104.2	2.0178	3.3
10.4	1.0170	58.3	1.7656	7.9	102.2	2.00945	5.3
11.2	1.0492	58.2	1.7649	8.0	102.1	2.00902	5.4

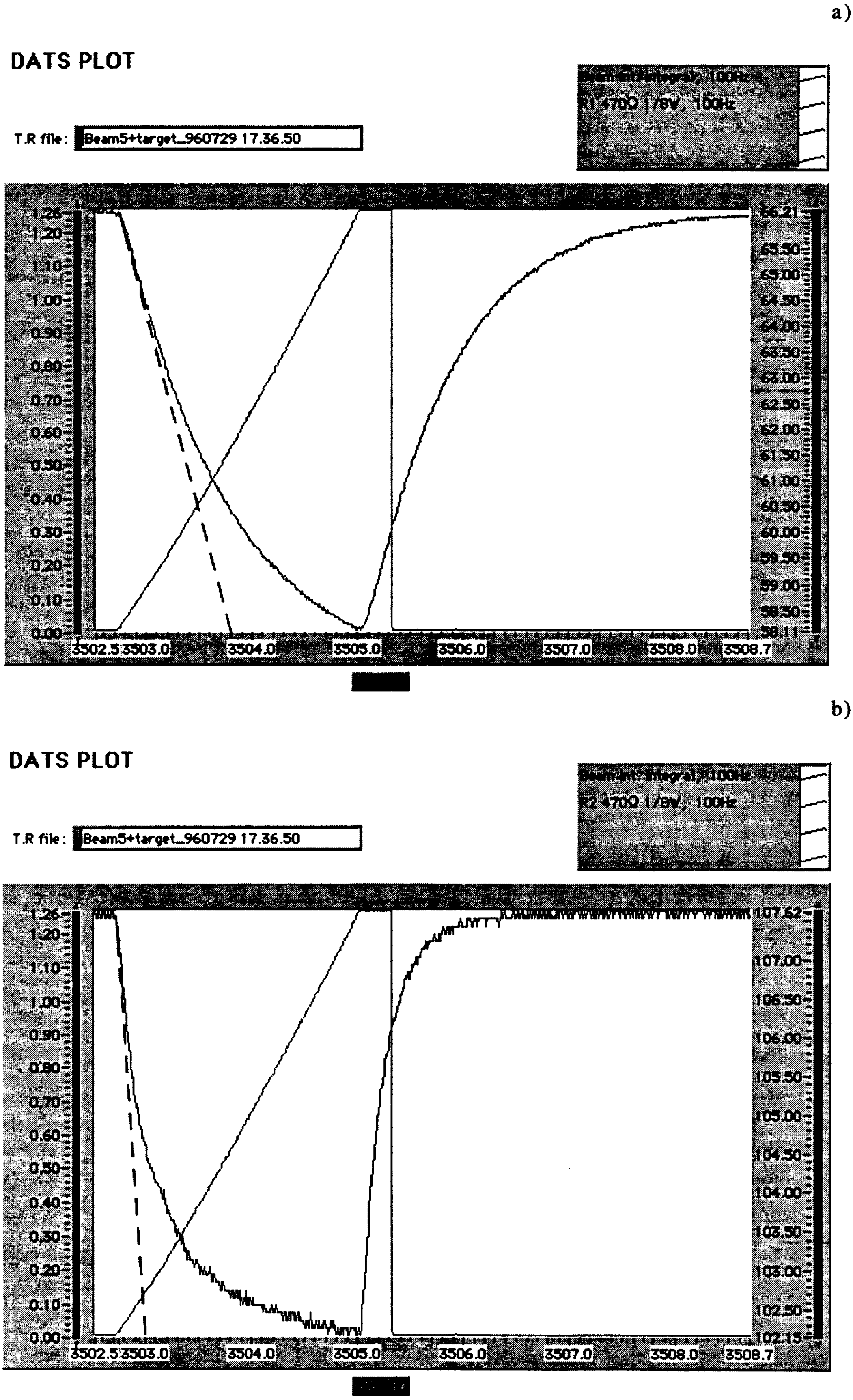

Fig. 12: a) Plot of *R* (*t*) and b) plot of R_s (*t*). The integrated number of protons incident on the target is $11.2 \cdot 10^7$. Left vertical axis: integrated number of protons (straight lines) in arbitrary units. Right vertical axis: resistance *R* or R_s in [kΩ] (exponential curves). Horizontal axis time *t* [s]. The spill duration is about 2.2 s.

a)

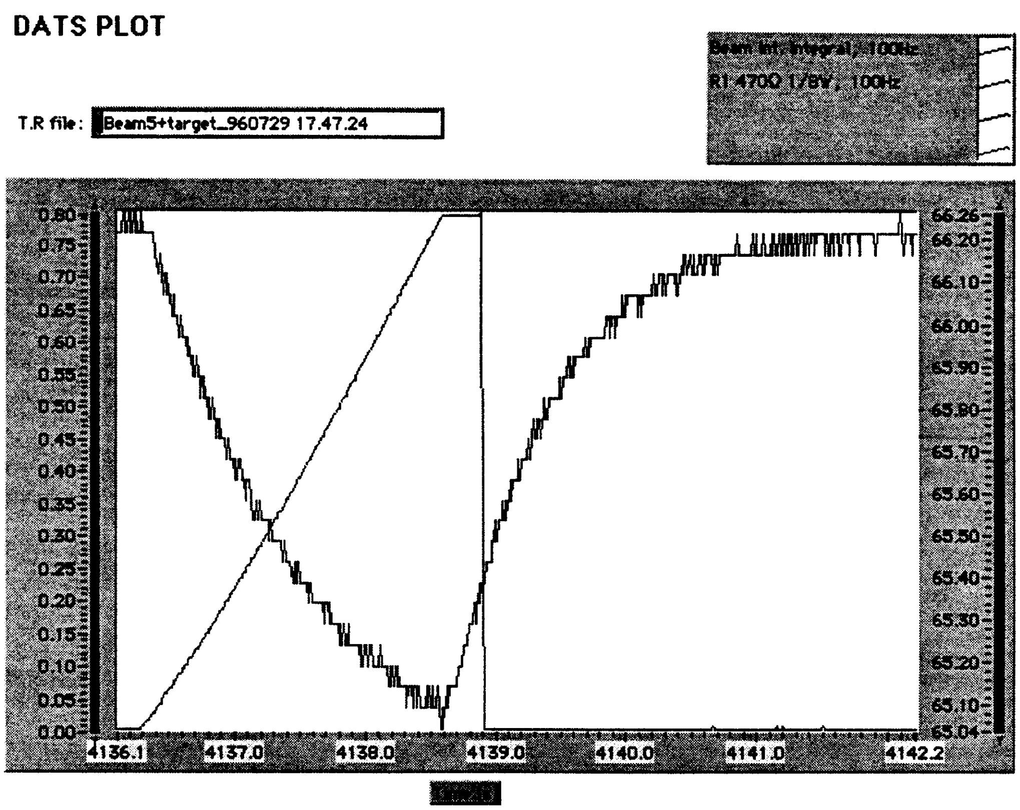

b)

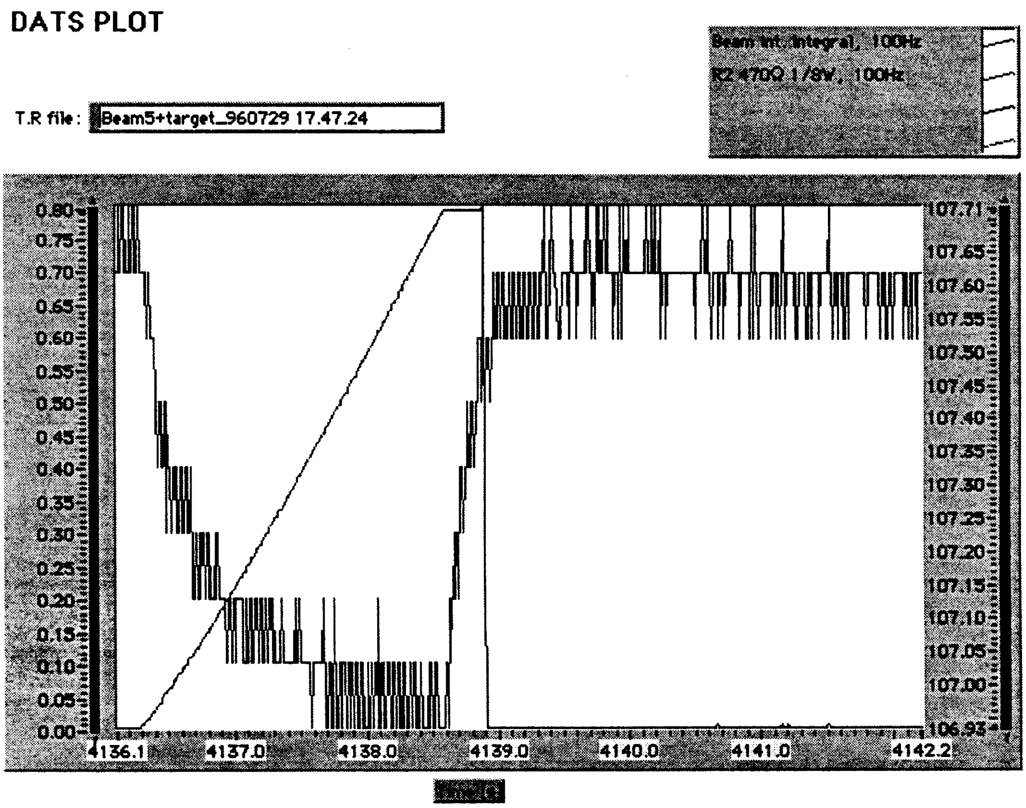

Fig. 13: a) Plot of $R(t)$ and b) plot of $R_s(t)$. The integrated number of protons incident on the target is $1.2 \cdot 10^7$. Left vertical axis: integrated number of protons in arbitrary units (straight lines). Right vertical axis: resistance R or R_s in [kΩ] (exponential curves). Horizontal axis: time t [s]. The spill duration is about 2.2 s.

Anticipating a future use of logarithmic amplifiers, intended to cover a few decades for the resistances and for the number of particles, a plot of log(R) versus log (number of protons) is given in:

- Fig. 14(a) where the full line represents log(R [kΩ]) as a function of log(N [10^7]) and the dotted line the linear regression line. The regression line follows the equation: log(R [kΩ]) = −0.053.log(N [10^7]) + 1.823. The correlation factor is $\sigma = -0.971$.
- Fig. 14(b) where the full line represents log(R_s [kΩ]) as a function of log(N [10^7]) and the dotted line the linear regression line. The regression line follows the equation: log(R_s [kΩ]) = −0.021.log(N [10^7]) + 2.033. The correlation factor is $\sigma = -0.961$.

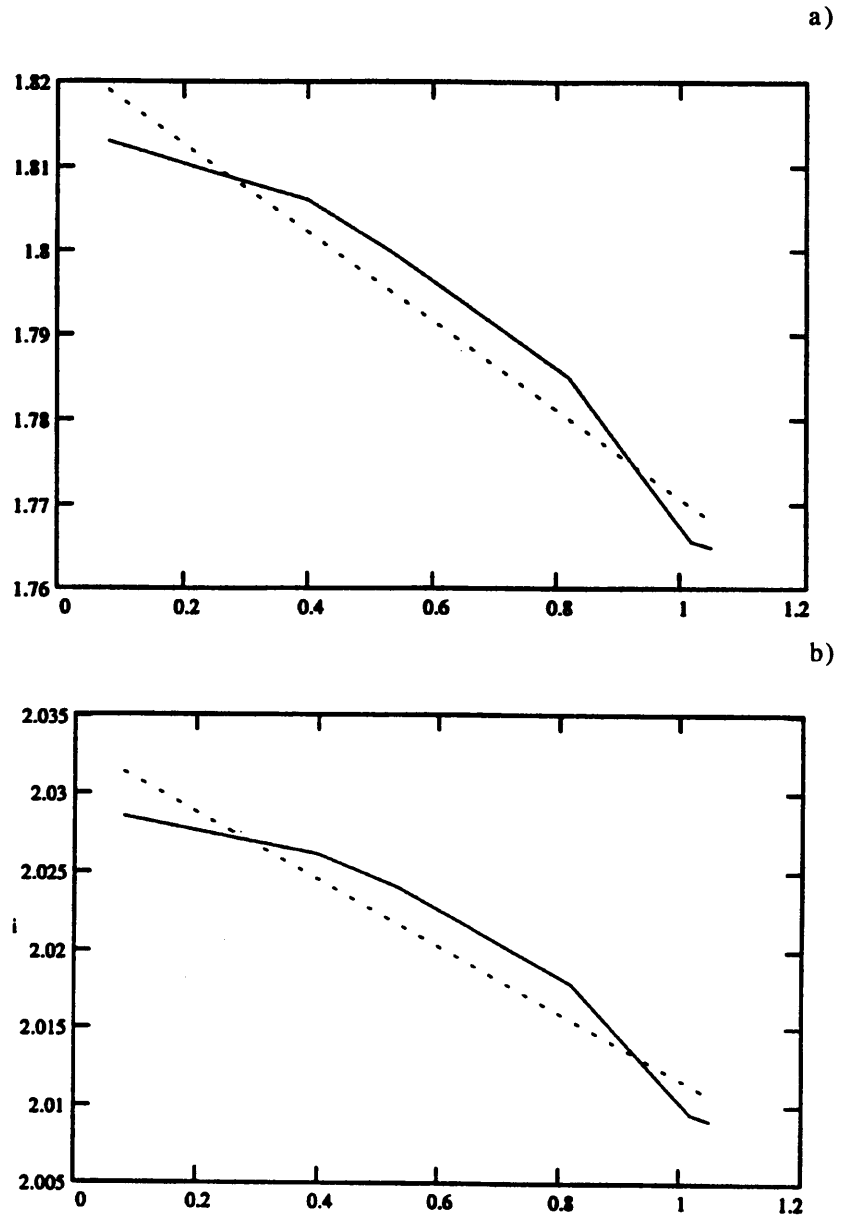

Fig. 14: a) Plot of log(R [kΩ]) as a function of log(N [10^7]); b) plot of log(R_s [kΩ]) as a function of log(N [10^7]) from Table 3.

3.2.3 *Estimates of the temperature increase ΔT*

We consider only the resistance R which, since associated with a relatively large copper volume, gives significant results.

From Table 3 and Eq. (1) used with the coefficients given in Section 2.4 e one can determine the actual resistance temperature increase: $\Delta T_m = T(R) - T_o(R)$, as a function of the number N of protons on the target.

On the other hand, in a quasi-theoretical way we use the procedure described in Section 3.1.2. One can thus consider the deposited heat rate of a well-aligned calorimeter from Fig. 9 as being about $1.5 \cdot 10^{-10}$ [J/kg·proton] such that:

$$\dot{Q}\,[\mathrm{J/g \cdot s}] = (1.5 \cdot 10^{-13}\ \mathrm{J/g \cdot proton}) \cdot (N\ \mathrm{protons/(spill\ time)})$$

with a spill time equal to 2.2 s. Now since $\Delta Q\,[\mathrm{J/g}] = \tau \cdot \Delta \dot{Q}$ where $\tau = 1$ s is the microcalorimeter time constant, one can make use of Eq. (3) with $T_{ic} = T_o(R)$ in order to determine the theoretical temperature increase ΔT_{th}.

One can argue that ΔT_{th} refers to a resistance which has reached its final asymptotic value. Therefore a correction has to be applied to R so as to use instead

$$R_{cor} = R_0 - \frac{(R_0 - R)}{1 - e^{-\alpha}} \quad \text{with} \quad \alpha = \frac{\text{spill time}}{\tau} = \frac{2.2}{1}\ .$$

The corrected measured temperature increase would then be: $\Delta T_{cor} = T(R_{cor}) - T_o(R)$.

The plot of ΔT_m, ΔT_{cor} and ΔT_{th} is given in Fig. 15. The relative differences between the three curves do not exceed a factor 2. Taking into account all the uncertainties (in the calibration of R, the energy deposition estimates, etc.) these results are quite satisfactory.

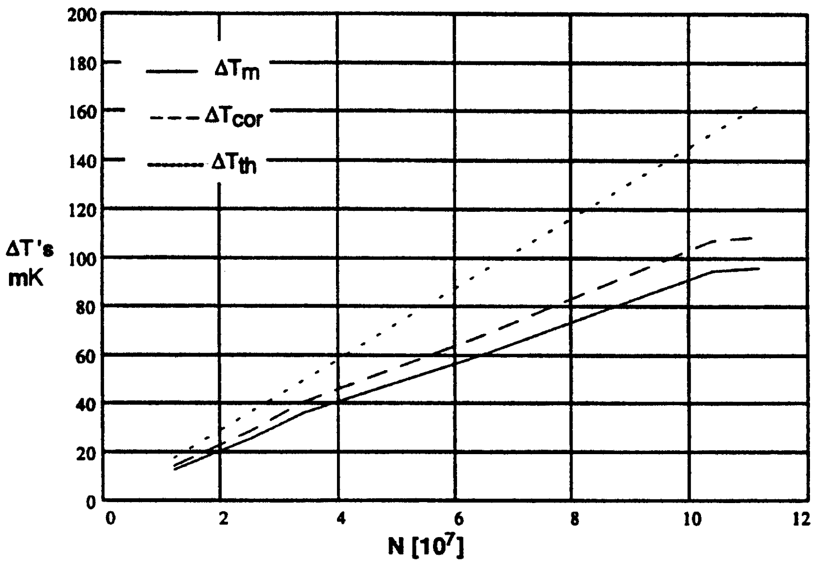

Fig. 15: Plot of ΔT_m, ΔT_{cor} and ΔT_{th} (small dotted curve) in mK as a function of the integrated number $N\,[10^7]$ of protons impinging on the target.

3.3 Rough estimates in connection with LHC proton beam losses

In the present state of our experiments we can estimate (see Section 3.2.1) that we can measure the energy deposited by: $3.4\cdot 10^5$ protons/s arriving on the target at 120 GeV/c. The deposited energy in the copper block for one proton on the target is, according to Fig. 9, $2\cdot 10^{-10}$ [J/kg].

As far as concerns the LHC a proton lost at 7 TeV will deposit at the level of the mucal (Ref. [2]): $1.6\cdot 10^{-10}$ [J/cm^3] and $1.4\cdot 10^{-11}$ [J/cm^3] at 0.45 TeV (Ref. [3]).

Let us express by $N_{\rm lhc}$ the number of protons lost per second which can be detectable at the present state of our experiments. A lower estimate is therefore:

$$\frac{1.6\cdot 10^{-10}}{8.96\ [\mathrm{g}\cdot \mathrm{cm}^{-3}]}\cdot N_{\rm lhc} = 3.4\cdot 10^5 \cdot 2\cdot 10^{-10}\cdot 10^{-3}$$

$$N_{\rm lhc} = 3.8\cdot 10^3 \text{ protons lost/s}\,.$$

On account of the uncertainty as to the point where the proton beam is lost, one has to increase this number such that one would instead consider $4\cdot 10^4$ protons lost/s. This has to be confirmed by future experiments.

It is worthwhile remembering that at 7.0 TeV an LHC main dipole will quench when submitted to a continuous loss of $7.8\cdot 10^6$ p/(m.s) and $7\cdot 10^8$ p/(m.s) at 0.45 TeV.

4 Conclusions

As expected we have shown that the principle of the microcalorimeter could be applied to the diagnostics of beam losses. A quite good relationship between the amount of 'lost' particles and the change of the thermometer resistance has been found for a proton beam whose intensity varies by a factor 10. In a later stage we should be concerned with several decades' variations.

As for the experiments made in the laboratory, they are quite coherent and can be compared with measurements made with extracted proton beams. Future tests should be oriented towards a better estimation of the physical thermal capacity and resistances represented in Fig. 4 in order to improve the microcalorimeter performance.

In the field of beam-loss detectors, we are investigating sensitive thermometers having short heating and cooling times. This has been obtained with the 1/8 W Allen-Bradley resistances. Some work towards a better heat transmission between the copper blocks and the resistance R and between the copper blocks and the cold source should be pursued in order to reach small response times while keeping large resistance variations. The influence of the copper volume on the overall performance has to be studied more accurately.

On the other hand, the investigation of resistances having large relative $|\mathrm{d}R/\mathrm{d}T|_{T=T_{\rm exp}}$ is essential.

Together with the above-mentioned future developments we also plan to improve the electronic circuits and the accuracy of the processing system.

Acknowledgements

We wish to thank J. Camas, J. Casas-Cubillos, R. Jung, L. Serio, M. Silari and G.R. Stevenson for their constant help and support.

References

[1] Cryogenic microcalorimeters for the measurement of energy deposition by beam losses in superconducting accelerator magnets, Ph. Lebrun, H. Blessing, T. Taylor and L. Walkiers, CERN AT/92-18 (CR-MA).

[2] Use of microcalorimeters as beam loss detectors, J. Bosser, PS/BD/Note 94–01.

[3] Quench levels and transient beam losses in LHC magnets, J.B. Jeanneret, D. Leroy, L. Oberli and T. Trenkler, LHC Project report 44.